Published in final edited form as:
J Neurosci Res. 2009 November 15; 87(15): 3502–3510. doi:10.1002/jnr.21984.

PROTEOMIC ANALYSIS OF OPTIC NERVE LIPID RAFTS REVEALS NEW PARANODAL PROTEINS

Yasuhiro Ogawa[†] and **Matthew N. Rasband**
Department of Neuroscience, Baylor College of Medicine, One Baylor Plaza, Houston, TX 77030

Abstract

Neuron-glia interactions at paranodal junctions play important roles in action potential propagation. Among their many functions, they contribute to the passive electrical properties of myelinated nerve fibers and actively regulate the polarized distribution of ion channels along axons. Despite their importance, relatively little is known about the molecules responsible for paranode formation and function. Paranodal junction formation apparently depends on interactions among three cell adhesion molecules: caspr and contactin on the axon, and neurofascin 155 (NF-155) on the glial membrane. Using *Caspr-null* paranodal mutant mice we demonstrate that loss of paranodal junctions causes failure of NF-155 to partition into lipid rafts, indicating that proteins located at paranodal junctions have biochemical characteristics of lipid raft associated proteins. Based on this property of paranodal junctions, we used mass-spectrometry of lipid rafts isolated from a pure white matter tract (optic nerve) to search for new paranodal proteins. Since we used a relatively crude biochemical preparation, we identified several hundred different proteins. Among these, we found all previously described paranodal proteins. Further analysis based on antibody staining of central and peripheral nerves revealed β-adducin, septin 2, and sh3p8 as putative paranodal proteins. We describe the localization of these proteins in relation to other markers of nodes, paranodes, and juxtaparanodes in adult and developing nerve fibers. Finally, we describe their distribution in dysmyelinating *TremblerJ* mice, a model for the peripheral neuropathy Charcot-Marie-Tooth disease.

Keywords

Myelin; node of Ranvier; axon; axoglial junction

Introduction

Myelinated axons are segregated into distinct domains that include the node of Ranvier, its flanking paranodal and juxtaparanodal regions, and the internode. Each domain is enriched in a unique set of ion channels, cell adhesion molecules (CAMs), and cytoskeletal and scaffolding proteins (Susuki and Rasband, 2008). The identification of proteins unique to each of these domains has shed considerable light on the mechanisms whereby they form and are regulated. For example, it is now clear that formation of all three domains depends on neuron-glia interactions initiated through CAMs (Poliak and Peles, 2003; Salzer, 2003; Schafer and Rasband, 2006). These CAMs in turn bind to cytoskeletal and scaffolding proteins such as ankyrins, spectrins, 4.1 proteins, and MAGUKs. Finally, these cytoskeletal

Address correspondence to: Dr. Matthew N. Rasband, Department of Neuroscience, Baylor College of Medicine, One Baylor Plaza, Houston, TX 77030, Rasband@bcm.edu, 713-798-4494.
[†]Dr. Ogawa's present address is: Meiji Pharmaceutical University, 2-522-1 Noshio, Kiyose, Tokyo 204-8588, Japan, Phone: +81-42-495-8403, Fax: +81-42-495-8403

proteins and scaffolds function to recruit and/or stabilize the ion channels necessary for action potential conduction.

Among these polarized axonal domains, only the paranode regulates the organization of the other domains. For example, mice lacking the cell adhesion molecules caspr or contactin fail to form proper paranodal junctions resulting in broadened Na+ channel clusters and juxtaparanodal proteins invading into paranodal zones (Bhat et al., 2001; Boyle et al., 2001; Poliak et al., 2001; Rasband et al., 2003; Rios et al., 2003). In the CNS, some evidence suggests that paranodal junctions initiate the clustering of Na+ channels (Rasband et al., 1999), and regulate the types of Na+ channels located in myelinated axons (Boiko et al., 2001). Indeed, one recent report by Zonta et al. (Zonta et al., 2008) demonstrated that paranodal junctions in the CNS were sufficient to initiate clustering of Na+ channels even in the absence of nodal neurofascin-186 (NF-186). Despite the importance of these structures, very little is known about their molecular organization. The CAM neurofascin-155 (NF-155) located on the paranodal glial membrane participates in *trans* interactions with the axonal CAMs caspr and contactin. These proteins are essential for paranode formation and maintenance since their ablation results in paranodal loops that do not attach to the axon and can even face away from the axonal membrane (Bhat et al., 2001; Boyle et al., 2001; Sherman et al., 2005). Paranodal CAMs appear to be stabilized at the paranodal junctions through interactions with 4.1 proteins. On the axonal side, protein 4.1B binds to caspr (Denisenko-Nehrbass et al., 2003), while on the glial side protein 4.1G has been reported at paranodes (Ohno et al., 2006). The binding partner of 4.1G has not been described although it may be NF-155. 4.1 proteins link to the actin-based cytoskeleton through spectrins and ankyrins. Recently, we used a biochemical fractionation strategy followed by mass-spectrometry to identify a specialized paranodal cytoskeleton consisting of αII spectrin, βII spectrin, and ankyrinB (Ogawa et al., 2006). Taken together, these observations indicate that despite their important roles in myelinated axons, little is known about the molecular organization of paranodal junctions.

Here, we report the results of a proteomic analysis of membrane fractions highly enriched in paranodal proteins. We describe three new paranodal proteins, their localization during developmental myelination, and their localization in the dysmyelinating mutant mouse *TremblerJ*.

Materials and Methods

Animals

Rat and mouse tissues were collected by rapidly dissecting out the tissue after killing animals with halothane. *Caspr-null* mice have been described previously (Gollan et al., 2003) and were kindly provided by Dr. Elior Peles (Weizmann Institute, Israel). *TremblerJ* mice were obtained from The Jackson Laboratories. All experiments were performed in accordance with the National Institutes of Health guidelines for the humane treatment of animals.

Antibodies

The mouse monoclonal Na+ channel, PanNF, caspr, Kv1.2, and βII spectrin antibodies have been described previously (Bekele-Arcuri et al., 1996; Rasband et al., 1999; Schafer et al., 2004; Ogawa et al., 2006). Rabbit anti-ZO-1 was purchased from Invitrogen. Mouse anti-2′3′ cyclic nucleotide phosphodiesterase (CNPase) was purchased from Sigma. Rabbit polyclonal β-adducin antibodies have been described (Gilligan et al., 1999) and were kindly provided by Dr. Diana M. Gilligan (University of Washington School of Medicine). Rabbit polyclonal anti-septin 2 antibodies were kindly provided by Dr. Shu-Chan Hsu (Rutgers

University). Rabbit polyclonal and mouse monoclonal anti-sh3p8 antibodies were kindly provided by Dr. James Trimmer (UC Davis) and purchased from Neuromab (www.neuromab.org), respectively.

Immunostaining

Immunostaining of optic and sciatic nerves was performed as described by Schafer et al. (Schafer et al., 2004). The myelin retraction experiment was performed as previously described (Ogawa et al., 2006).

Isolation of lipid raft and mass-spectrometry

Biochemical analysis of NF-155 solubility and association with lipid rafts was performed as described (Schafer et al., 2004). We pooled mouse brain membrane homogenates from two WT mouse and 2 Caspr-null mouse brains for the analysis of NF-155 solubility. For the preparation of lipid rafts to be analyzed by mass-spectrometry we used ~80 rat optic nerves. Mass-spectrometry was performed at the University of Connecticut Health Center as described (Ogawa et al., 2006).

Results

Lipid rafts are enriched in paranodal proteins

Paranodal neuron-glia interactions are mediated by three different cell adhesion molecules (CAMs) including axonal caspr and contactin, and the glial 155 kD form of neurofascin (NF-155). Previous studies have demonstrated that these three proteins are associated with detergent insoluble protein complexes that float at low densities on sucrose gradients (i.e. lipid rafts; Schaeren-Wiemers et al., 2004; Schafer et al., 2004). Schafer et al., (2004) showed that NF-155 acquires these biochemical properties concomitant with the assembly of the paranodal junction. If an intact paranodal junction is required for recruitment of NF-155 into the lipid raft, then paranodal mutant mice should lack NF-155 in lipid rafts isolated from their brain membranes. To test this hypothesis, we prepared crude brain membranes from adult caspr-null (caspr KO) and wild-type (WT) littermate mice. Although these animals have similar amounts of NF-155 and NF-186 (Fig. 1A), in contrast to WT mice NF-155 from caspr-null mice was soluble in 1% TX-100 at 4°C (compare insoluble pellet (P) fractions in Fig. 1A). Furthermore, NF-155 was almost completely eliminated from lipid raft fractions isolated on sucrose gradients (Fig. 1B). Thus, loss of caspr-dependent paranodal neuron-glia interactions blocks the recruitment of NF-155 into lipid rafts.

The clear association of NF-155, caspr, and contactin with lipid rafts suggested that isolating lipid rafts from pure white matter tracts might be an effective method to purify the protein components associated with paranodes. To this end we collected rat optic nerves, made a crude membrane homogenate, then isolated the lipid rafts on a sucrose gradient. We pooled fractions 3-5 (Fig. 1C) and size fractionated the proteins by 1-dimensional SDS-PAGE. The proteins were then excised from the gel and identified using liquid chromatography/tandem mass-spectrometry. This analysis resulted in the identification of several hundred different proteins (table 1 and supplemental table 1). Among these were known paranodal proteins including caspr, contactin, neurofascin, and protein 4.1B (Supplemental Table 1). We also identified ankyrinB, αII spectrin, and βII spectrin, consistent with our previous description of a specialized paranodal cytoskeleton (Ogawa et al., 2006).

In addition to known paranodal proteins, we found myelin proteins (e.g. myelin basic protein (MBP), myelin associated glycoprotein (MAG), etc.), juxtaparanodal proteins (e.g. Kv1.1 and TAG-1), and many other proteins with unknown functions in myelinated nerves (Table 1). The heterogeneity of proteins identified was not surprising since we also purified

lipid rafts not associated with paranodal junctions, but derived from oligodendrocytes, astrocytes, NG2 glia, and axons.

Identification of new paranodal proteins

To identify proteins enriched at paranodes, we next obtained antibodies against proteins identified by mass-spectrometry. We used these antibodies to immunolabel optic and sciatic nerves. Among the many antibodies we screened (data not shown) we found β-adducin, septin2, and sh3p8 as putative paranodal proteins (Table S1). We describe immunolocalization experiments for each of these proteins below. Evaluation of the many additional proteins identified by mass-spectrometry will require additional experiments since not all proteins have readily available antibodies and some antibodies were not of sufficient quality to determine the distribution of its target antigen.

β-adducin

Adducins facilitate the association of spectrins with actin and are thought to participate in recruiting diverse proteins to actin filament ends (Bennett et al., 1988; Bennett and Baines, 2001). This function is consistent with the recent identification of a paranodal cytoskeleton enriched in both αII and βII spectrin (Ogawa et al., 2006). In adult myelinated optic nerve axons β-adducin staining flanked nodes of Ranvier in paranodal and juxtaparanodal regions. This distribution is very similar to that observed for βII spectrin (Fig. 2A) and protein 4.1B (Ogawa et al., 2006). A similar distribution for β-adducin was found in adult sciatic nerve, with significant colocalization between β-adducin and βII spectrin (Fig. 2B). The paranodal localization of β-adducin was much more prominent during developmental myelination in the PNS. β-adducin was clearly enriched at forming paranodal junctions where it colocalized with Caspr and Kv1 channels (Fig. 2C). At postnatal day 2 (P2), β-adducin was not detectable, consistent with the fact that in the PNS paranodal junctions mature after Na+ channel clustering (Schafer et al., 2006). However, by P4, clear paranodal β-adducin could be detected. At P8 and P15 β-adducin was clearly enriched at paranodal junctions where it colocalized with caspr immunoreactivity. In many fibers, this immunoreactivity extended into juxtaparanodal domains where it colocalized with Kv1.2 (Fig. 2C).

To begin to identify the function of β-adducin we obtained nervous system tissues from β-adducin knockout mice (Rabenstein et al., 2005). However, immunostaining of these animals failed to reveal any paranodal abnormalities (YO and MNR unpublished results). One possible explanation for this may be compensation by other adducins including α- or γ-adducin.

Septin 2

Septin 2 is a member of the septin family of cytoskeletal GTP-binding proteins. They have been reported to participate in many cellular functions including cell division, trafficking of organelles, and regulation of actin filaments (Kinoshita et al., 2002). Previous proteomic studies on myelin revealed Septin 7 as a putative paranodal protein (Roth et al., 2006), and septins 2, 6, and 7 are thought to co-assemble (Kinoshita et al., 2002). We used antibodies against septin 2 to immunostain adult and developing sciatic nerve. In adult nerves we found septin 2 enriched at paranodal junctions flanking nodal Na+ channels (Fig. 3A) and colocalized with paranodal neurofascin (Fig. 3B). Septin 2 immunostaining was restricted to the paranodal junctions and did not colocalize with juxtaparanodal Kv1 channels (Fig. 3D). Importantly, we also found high levels of actin enriched at paranodal junctions, consistent with the reported role of septin 2 in regulating actin filaments (Fig. 3D). A developmental analysis of septin 2 localization during myelination revealed prominent immunofluorescence staining at developing paranodal junctions, with the highest levels of septin 2

immunoreactivity detected at P4 (Fig. 3E). The septin 2 immunoreactivity flanked nodal Na + channels, and colocalized with the paranodal proteins caspr and ZO-1.

sh3p8

Sh3p8 (also known as endophilin 2 and sh3gl1) is a protein thought to be involved in vesicle recycling and endocytosis, and forms complexes with synaptojanin and dynamin I (Ringstad et al., 1997); dynamin I, clathrin, epsin2, and other vesicular trafficking proteins were also identified in our screen - see Table S1). Immunostaining of sciatic nerve using antibodies against sh3p8 revealed a clear paranodal distribution for the protein (Fig. 4A). We confirmed that two different rabbit polyclonal and mouse monoclonal antibodies against sh3P8 could label paranodes (data not shown). However, in contrast to septin 2 and β-adducin, the immunoreactivity was often located on the outer aspect of the Schwann cell membrane and not just at the paranodal junction (although in many instances the immunoreactivity colocalized with markers of the paranodal junction e.g. Fig 4A), suggesting that sh3p8 is found in the Schwann cell. We used antibodies against ZO-1 to label the paranodal autotypic tight junctions and compared this to the staining pattern for sh3p8 (compare Figs. 4A and 4B). To confirm the localization of sh3p8 to the Schwann cell membrane we treated unfixed, teased sciatic nerve fibers using sequential rounds of hyper- and hypotonic sucrose solutions, to loosen paranodal junctions, followed by enzymatic digestion by collagenase. This resulted in the retraction of the Scwhann cell membranes away from the node of Ranvier. Immunostaining demonstrated that the sh3p8 immunoreactivity was displaced from the paranodes after retraction of the Schwann cell membranes, confirming that sh3p8 is located in the Schwann cell (Fig. 4C). We performed a developmental analysis of sh3p8 in the sciatic nerve and found that it was restricted to paranodal regions of myelinating Schwann cells where it flanked Na+ channels or overlapped (but did not precisely colocalize) with markers of the paranodal junction including caspr, ZO-1, and 2′,3′-cyclic nucleotide phosphodiesterase (CNPase) (Fig. 4D). For example, at P4, sh3p8 immunoreactivity did not precisely colocalize with caspr staining and instead appeared in a more internodal distribution reminiscent of juxtaparanodal staining. The significance of this redistribution is unknown, but is similar to the developmental changes in distribution observed for the paranodal cytoskeletal protein ankB (Ogawa et al., 2006).

Localization of new paranodal proteins in TremblerJ dysmyelinated nerve fibers

TremblerJ (TrJ) mice have been used as a model to study the effects of peripheral nerve dysmyelination on the organization of ion channels within axonal membrane domains (Devaux and Scherer, 2005). These mice undergo repeated bouts of demyelination and remyelination, resulting in Kv1 channels, normally restricted to juxtaparanodes, that can be found in paranodal regions, suggesting disrupted or improperly formed paranodal junctions (Devaux and Scherer, 2005). To evaluate the consequence of dysmyelination and paranode disruption on the localization of β-adducin, septin 2, and sh3p8, we immunostained sciatic nerves from *TrJ* mice (Fig. 5). As described, β-adducin was found in both paranodal and juxtaparanodal domains of WT littermates (Figs. 5A, 5B), whereas septin 2 (Fig. 5C, 5D) and sh3p8 (Fig. 5E, 5F) were restricted to paranodal regions. In *TrJ* mice β-adducin could be found all along the axon, occasionally dramatic enrichment at paranodal or juxtaparanodal regions could be seen (Fig. 5A). The most pronounced feature of the β-adducin staining was a clear gap in immunoreactivity at the nodes of Ranvier (Fig. 5B). This gap likely represents the high density of Na+ channels and its associated cytoskeleton consisting of ankyrinG and βIV spectrin. Septin 2 staining in *TrJ* mice revealed that even in paranodal junctions that were clearly disrupted based on their disorganized caspr immunoreactivity, septin 2 colocalized with caspr. This result suggests that septin 2 strongly interacts with the caspr-containing paranodal protein complex. Even when Kv1 channels were not detected, septin 2

could be identified (Fig. 5D). Sh3p8 immunostaining in *TrJ* mice did not always correlate well with the detection of paranodal junctions. In many cases, although caspr could be detected flanking both sides of the node of Ranvier, sh3p8 immunoreactivity was found only on one side of the node (Fig. 5E, 5F). In some instances, sh3p8 immunoreactivity appeared in more internodal and juxtaparanodal regions as opposed to paranodal zones, similar to what was observed during developmental myelination (Fig. 4D).

Discussion

Biochemical fractionation and proteomic analysis of myelinated nerve fibers has been used successfully to determine the molecular composition of myelin (Taylor et al., 2004; Huang et al., 2005; Roth et al., 2006). The purpose of the work reported here was to further fractionate myelinated axons into paranodal and non-paranodal fractions, based on the fact that paranodal proteins co-fractionate with lipid rafts (Schafer et al., 2004), then use mass-spectrometry to identify proteins associated with the paranodal junction. We previously used this strategy successfully to elucidate the existence of a paranodal cytoskeleton consisting of αII spectrin, βII spectrin, and ankyrinB (Ogawa et al., 2006). We used the rat optic nerve, a pure white matter tract, as starting material in order to eliminate contamination of our paranodal lipid raft fractions by post-synaptic densities (PSDs), which also have biochemical characteristics of lipid rafts (Hering et al., 2003). Despite the absence of PSDs, we still identified many proteins that are unlikely to be components of paranodal junctions. This is probably due to isolation of rafts from other cell types and locations in the optic nerve such as astrocytes and axonal internodes, respectively. Nevertheless, the strategy was successful since we identified nearly every previously described paranodal junction protein, as well as three new components: β-adducin, septin 2, and sh3p8. Additional experiments will be needed to test the many other potential candidate proteins listed in supplementary table 1 to determine if they are bona fide paranodal proteins.

Among the many proteins we identified, relatively few membrane proteins were represented. Whether this is a limitation of the methodology, or an accurate picture of the lipid rafts found in optic nerve is not known. The majority of paranodal junction proteins that have been described are located in the axon. Very few proteins have been shown to be located on the glial side of the paranodal junction; to the best of our knowledge, only Neurofascin-155, protein 4.1G, and stathmin, a microtubule destabilizing protein, have been reported at the paranodal junction (Tait et al., 2000; Southwood et al., 2004; Ohno et al., 2006), although several other proteins have been described at the paranodal loops and/or autotypic tight junctions of oligodendrocytes and/or Schwann cells (Gow et al., 1999; Poliak et al., 2002; Nie et al., 2003; Southwood et al., 2007); for a review see (Spiegel and Peles, 2002).

Based on the immunofluorescence staining shown here, β-adducin, septin 2, and sh3p8 all appeared to be present at the paranodal junction, although sh3p8 had a more prominent distribution consistent with a localization to the autotypic tight junctions of Schwann cells. A definitive description of their localization will require the availability of more robust antibodies whose antigens survive the harsh fixation conditions necessary for immunoelectron microscopy.

In this report we focused primarily on the description of new paranodal proteins and their localization in mature, developing, and remyelinating nerve fibers. To determine the function of β-adducin we examined CNS and PNS myelinated nerve fibers from mice lacking β-adducin (Rabenstein et al., 2005), however we did not observe any paranodal abnormalities (YO and MNR unpublished results). It is possible that compensation occurs at the paranodal junction since other adducins are present in the nervous system, and adducins form heteromers of α- and β- or α- and γ-subunits (Hughes and Bennett, 1995). Recently,

mice deficient in α-adducin were shown to lack β- and γ-adducin in red blood cells, leading to hemolytic anemia due to spherocytosis (Robledo et al., 2008). These animals also had profound CNS abnormalities including hydrocephalus. It will be important to evaluate these animals for paranode disruption, and to generate mice deficient in both α and β-adducins. Moreover, adducins are required for membrane stailization in epithelial cells through spectrin interactions (Abdi and Bennett, 2008). Thus an alternative role for β-adducin might be to stabilize the paranodal junction. In this case, paranodal phenotypes might only appear in aged β-adducin null mice.

Septin 2 is thought to be an important regulator of actin dynamics and the cytoskeleton. Consistent with this idea we showed that paranodal regions of myelinated nerve fibers are also enriched in actin, which in turn is linked to paranodal membrane proteins through αII/βII spectrin tetramers and the scaffolding proteins ankB and protein 4.1B (Ogawa et al., 2006). Mice that fail to form proper paranodal neuron-glia interactions have a disrupted paranodal cytoskeleton and undergo axon degeneration (Garcia-Fresco et al., 2006). Since our experiments cannot resolve whether septin 2 is axonal or glial, it is possible that septin 2 contributes to cytoskeleton organization in the paranodal loops of myelinating glia. However, silencing of septin 2 expression in cultured Schwann cells did not affect cell morphology. Similarly transfection of myelinating Schwann cells with a nonfunctional form of septin 2 did not affect the paranodal cytoskeleton (YO and MNR unpublished results). Future experiments to determine the function of septin 2 will require silencing septin 2 expression during development in axons and separately in Schwann cells.

The enrichment of sh3p8 at paranodal regions of Schwann cells is intriguing since this protein is thought to be involved in vesicle recycling and endocytosis. However, paranodal and autotypic tight junctions have not been previously reported to be sites of active vesicle recycling. Besides the paranodes, we found high levels of sh3p8 and its binding partners in Schmitt-Lantermann (SL) incisures (YO and MNR unpublished results). Like paranodes, SL incisures are sites of autotypic tight junctions and cytoplasmic channels that traverse between adaxonal and abaxonal compartments of the schwann cell. Although it is unclear whether endocytosis regulates myelin membrane stability, we speculate that the localization of sh3p8 to paranodes and SL incisures indicates that these may be sites of active membrane turnover.

In summary, the experiments described here demonstrate that paranodal proteins can be enriched and identified from lipid raft fractions of myelinated nerve fibers using proteomic tools like mass-spectrometry. Furthermore, lipid raft domains are thought to be important sites for signal transduction cascades and cellular signaling events. Our results reveal three new proteins that may be involved in these paranodal neuron-glia signaling interactions. However, our experiments also revealed two important limitations of the approach: 1) many proteins were identified that are not located at paranodes, and 2) when proteins are confirmed as paranodal proteins, careful follow-up experiments are required to determine their functions. While the first limitation can be overcome through adding steps to further purify paranodal proteins (e.g. affinity chromatography or additional fractionation on density gradients), determining the functions of paranodal proteins will require the concerted efforts of many neuroscientists utilizing diverse genetic, molecular and cellular methods. To this end the importance of these junctions for proper nervous system function should be strong motivation.

Supplementary Material

Refer to Web version on PubMed Central for supplementary material.

Acknowledgments

This work is dedicated to the memory of our friend, mentor, and colleague Dr. Steven Pfeiffer. Supported by National Institutes of Health grant NS044916, Mission Connect, and a grant from the Dr. Miriam and Sheldon G. Adelson Medical Research Foundation. YO is a postdoctoral fellow of the National Multiple Sclerosis Society. MNR is a Harry Weaver Neuroscience Scholar of the National Multiple Sclerosis Society.

References

Abdi KM, Bennett V. Adducin promotes micrometer-scale organization of beta2-spectrin in lateral membranes of bronchial epithelial cells. Mol Biol Cell. 2008; 19:536–545. [PubMed: 18003973]

Bekele-Arcuri Z, Matos MF, Manganas L, Strassle BW, Monaghan MM, Rhodes KJ, Trimmer JS. Generation and characterization of subtype-specific monoclonal antibodies to K+ channel alpha- and beta-subunit polypeptides. Neuropharmacology. 1996; 35:851–865. [PubMed: 8938716]

Bennett V, Baines AJ. Spectrin and ankyrin-based pathways: metazoan inventions for integrating cells into tissues. Physiol Rev. 2001; 81:1353–1392. [PubMed: 11427698]

Bennett V, Gardner K, Steiner JP. Brain adducin: a protein kinase C substrate that may mediate site-directed assembly at the spectrin-actin junction. J Biol Chem. 1988; 263:5860–5869. [PubMed: 2451672]

Bhat MA, Rios JC, Lu Y, Garcia-Fresco GP, Ching W, St Martin M, Li J, Einheber S, Chesler M, Rosenbluth J, Salzer JL, Bellen HJ. Axon-glia interactions and the domain organization of myelinated axons requires neurexin IV/Caspr/Paranodin. Neuron. 2001; 30:369–383. [PubMed: 11395000]

Boiko T, Rasband MN, Levinson SR, Caldwell JH, Mandel G, Trimmer JS, Matthews G. Compact myelin dictates the differential targeting of two sodium channel isoforms in the same axon. Neuron. 2001; 30:91–104. [PubMed: 11343647]

Boyle ME, Berglund EO, Murai KK, Weber L, Peles E, Ranscht B. Contactin orchestrates assembly of the septate-like junctions at the paranode in myelinated peripheral nerve. Neuron. 2001; 30:385–397. [PubMed: 11395001]

Denisenko-Nehrbass N, Oguievetskaia K, Goutebroze L, Galvez T, Yamakawa H, Ohara O, Carnaud M, Girault JA. Protein 4.1B associates with both Caspr/paranodin and Caspr2 at paranodes and juxtaparanodes of myelinated fibres. Eur J Neurosci. 2003; 17:411–416. [PubMed: 12542678]

Devaux JJ, Scherer SS. Altered ion channels in an animal model of Charcot-Marie-Tooth disease type IA. J Neurosci. 2005; 25:1470–1480. [PubMed: 15703401]

Garcia-Fresco GP, Sousa AD, Pillai AM, Moy SS, Crawley JN, Tessarollo L, Dupree JL, Bhat MA. Disruption of axo-glial junctions causes cytoskeletal disorganization and degeneration of Purkinje neuron axons. Proc Natl Acad Sci U S A. 2006; 103:5137–5142. [PubMed: 16551741]

Gilligan DM, Lozovatsky L, Gwynn B, Brugnara C, Mohandas N, Peters LL. Targeted disruption of the beta adducin gene (Add2) causes red blood cell spherocytosis in mice. Proc Natl Acad Sci U S A. 1999; 96:10717–10722. [PubMed: 10485892]

Gollan L, Salomon D, Salzer JL, Peles E. Caspr regulates the processing of contactin and inhibits its binding to neurofascin. J Cell Biol. 2003; 163:1213–1218. [PubMed: 14676309]

Gow A, Southwood CM, Li JS, Pariali M, Riordan GP, Brodie SE, Danias J, Bronstein JM, Kachar B, Lazzarini RA. CNS myelin and sertoli cell tight junction strands are absent in Osp/claudin-11 null mice. Cell. 1999; 99:649–659. [PubMed: 10612400]

Hering H, Lin CC, Sheng M. Lipid rafts in the maintenance of synapses, dendritic spines, and surface AMPA receptor stability. J Neurosci. 2003; 23:3262–3271. [PubMed: 12716933]

Huang JK, Phillips GR, Roth AD, Pedraza L, Shan W, Belkaid W, Mi S, Fex-Svenningsen A, Florens L, Yates JR 3rd, Colman DR. Glial membranes at the node of Ranvier prevent neurite outgrowth. Science. 2005; 310:1813–1817. [PubMed: 16293723]

Hughes CA, Bennett V. Adducin: a physical model with implications for function in assembly of spectrin-actin complexes. J Biol Chem. 1995; 270:18990–18996. [PubMed: 7642559]

Kinoshita M, Field CM, Coughlin ML, Straight AF, Mitchison TJ. Self- and actin-templated assembly of Mammalian septins. Dev Cell. 2002; 3:791–802. [PubMed: 12479805]

Nie DY, Zhou ZH, Ang BT, Teng FY, Xu G, Xiang T, Wang CY, Zeng L, Takeda Y, Xu TL, Ng YK, Faivre-Sarrailh C, Popko B, Ling EA, Schachner M, Watanabe K, Pallen CJ, Tang BL, Xiao ZC. Nogo-A at CNS paranodes is a ligand of Caspr: possible regulation of K(+) channel localization. Embo J. 2003; 22:5666–5678. [PubMed: 14592966]

Ogawa Y, Schafer DP, Horresh I, Bar V, Hales K, Yang Y, Susuki K, Peles E, Stankewich MC, Rasband MN. Spectrins and ankyrinB constitute a specialized paranodal cytoskeleton. J Neurosci. 2006; 26:5230–5239. [PubMed: 16687515]

Ohno N, Terada N, Yamakawa H, Komada M, Ohara O, Trapp BD, Ohno S. Expression of protein 4.1G in Schwann cells of the peripheral nervous system. J Neurosci Res. 2006

Poliak S, Peles E. The local differentiation of myelinated axons at nodes of Ranvier. Nature Reviews Neuroscience. 2003; 4:968–980.

Poliak S, Matlis S, Ullmer C, Scherer SS, Peles E. Distinct claudins and associated PDZ proteins form different autotypic tight junctions in myelinating Schwann cells. J Cell Biol. 2002; 159:361–372. [PubMed: 12403818]

Poliak S, Gollan L, Salomon D, Berglund EO, Ohara R, Ranscht B, Peles E. Localization of Caspr2 in myelinated nerves depends on axon-glia interactions and the generation of barriers along the axon. J Neurosci. 2001; 21:7568–7575. [PubMed: 11567047]

Rabenstein RL, Addy NA, Caldarone BJ, Asaka Y, Gruenbaum LM, Peters LL, Gilligan DM, Fitzsimonds RM, Picciotto MR. Impaired synaptic plasticity and learning in mice lacking beta-adducin, an actin-regulating protein. J Neurosci. 2005; 25:2138–2145. [PubMed: 15728854]

Rasband MN, Taylor CM, Bansal R. Paranodal transverse bands are required for maintenance but not initiation of Nav1.6 sodium channel clustering in CNS optic nerve axons. Glia. 2003; 44:173–182. [PubMed: 14515333]

Rasband MN, Peles E, Trimmer JS, Levinson SR, Lux SE, Shrager P. Dependence of nodal sodium channel clustering on paranodal axoglial contact in the developing CNS. Journal of Neuroscience. 1999; 19:7516–7528. [PubMed: 10460258]

Ringstad N, Nemoto Y, De Camilli P. The SH3p4/Sh3p8/SH3p13 protein family: binding partners for synaptojanin and dynamin via a Grb2-like Src homology 3 domain. Proc Natl Acad Sci U S A. 1997; 94:8569–8574. [PubMed: 9238017]

Rios JC, Rubin M, St Martin M, Downey RT, Einheber S, Rosenbluth J, Levinson SR, Bhat M, Salzer JL. Paranodal interactions regulate expression of sodium channel subtypes and provide a diffusion barrier for the node of Ranvier. J Neurosci. 2003; 23:7001–7011. [PubMed: 12904461]

Robledo RF, Ciciotte SL, Gwynn B, Sahr KE, Gilligan DM, Mohandas N, Peters LL. Targeted deletion of {alpha}-adducin results in absent {beta}- and {gamma}-adducin, compensated hemolytic anemia, and lethal hydrocephalus in mice. Blood. 2008

Roth AD, Ivanova A, Colman DR. New observations on the compact myelin proteome. Neuron Glia Biol. 2006; 2:15–21. [PubMed: 18634588]

Salzer JL. Polarized domains of myelinated axons. Neuron. 2003; 40:297–318. [PubMed: 14556710]

Schaeren-Wiemers N, Bonnet A, Erb M, Erne B, Bartsch U, Kern F, Mantei N, Sherman D, Suter U. The raft-associated protein MAL is required for maintenance of proper axon--glia interactions in the central nervous system. J Cell Biol. 2004; 166:731–742. [PubMed: 15337780]

Schafer DP, Rasband MN. Glial regulation of the axonal membrane at nodes of Ranvier. Curr Opin Neurobiol. 2006; 16:508–514. [PubMed: 16945520]

Schafer DP, Custer AW, Shrager P, Rasband MN. Early events in node of Ranvier formation during myelination and remyelination in the PNS. Neuron Glia Biol. 2006; 2:69–79. [PubMed: 16652168]

Schafer DP, Bansal R, Hedstrom KL, Pfeiffer SE, Rasband MN. Does paranode formation and maintenance require partitioning of neurofascin 155 into lipid rafts? J Neurosci. 2004; 24:3176–3185. [PubMed: 15056697]

Sherman DL, Tait S, Melrose S, Johnson R, Zonta B, Court FA, Macklin WB, Meek S, Smith AJ, Cottrell DF, Brophy PJ. Neurofascins are required to establish axonal domains for saltatory conduction. Neuron. 2005; 48:737–742. [PubMed: 16337912]

Southwood C, He C, Garbern J, Kamholz J, Arroyo E, Gow A. CNS myelin paranodes require Nkx6-2 homeoprotein transcriptional activity for normal structure. J Neurosci. 2004; 24:11215–11225. [PubMed: 15601927]

Southwood CM, Peppi M, Dryden S, Tainsky MA, Gow A. Microtubule deacetylases, SirT2 and HDAC6, in the nervous system. Neurochem Res. 2007; 32:187–195. [PubMed: 16933150]

Spiegel I, Peles E. Cellular junctions of myelinated nerves (Review). Mol Membr Biol. 2002; 19:95–101. [PubMed: 12126235]

Susuki K, Rasband MN. Spectrin and ankyrin-based cytoskeletons at polarized domains in myelinated axons. Exp Biol Med. 2008; 233:394–400.

Tait S, Gunn-Moore F, Collinson JM, Huang J, Lubetzki C, Pedraza L, Sherman DL, Colman DR, Brophy PJ. An oligodendrocyte cell adhesion molecule at the site of assembly of the paranodal axo-glial junction. J Cell Biol. 2000; 150:657–666. [PubMed: 10931875]

Taylor CM, Marta CB, Claycomb RJ, Han DK, Rasband MN, Coetzee T, Pfeiffer SE. Proteomic mapping provides powerful insights into functional myelin biology. Proc Natl Acad Sci U S A. 2004; 101:4643–4648. [PubMed: 15070771]

Zonta B, Tait S, Melrose S, Anderson H, Harroch S, Higginson J, Sherman DL, Brophy PJ. Glial and neuronal isoforms of Neurofascin have distinct roles in the assembly of nodes of Ranvier in the central nervous system. J Cell Biol. 2008; 181:1169–1177. [PubMed: 18573915]

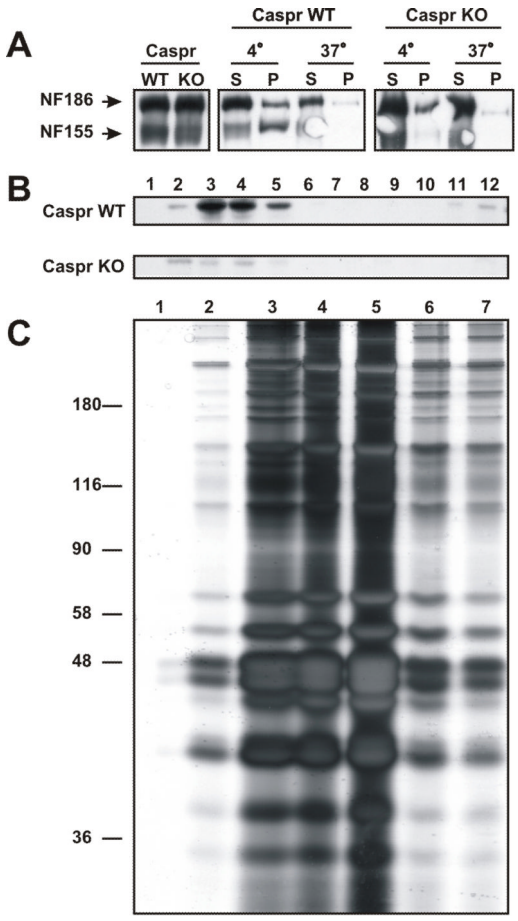

Figure 1.

Paranodal proteins are enriched in lipid rafts. ***A,*** Immunoblot analysis of neurofascin expression in wild-type (WT) and *caspr-null* (KO) mice. The differential solubility of NF-155 and NF-186 in 1% TX-100 at 4°C and 37°C demonstrates that NF-155 is soluble in brain membranes from KO mice. ***B,*** Sucrose gradients from caspr WT and caspr KO mouse brain membranes assayed for NF-155 by immunoblot. NF-155 is absent from the raft fraction in the *Caspr-null* rafts. For **A** and **C**, brain membrane homogenates from two WT and two *caspr-null* mice were pooled, then used to perform the analysis of NF-155 solubility and association with lipid rafts. **C,** Silver-stain of proteins found in rat optic nerve lipid rafts; ~80 rat optic nerves were used to prepare the lipid rafts. Fractions 3-5 were pooled for subsequent size fractionation by 1-D SDS-PAGE and subsequent analysis by mass-spectrometry.

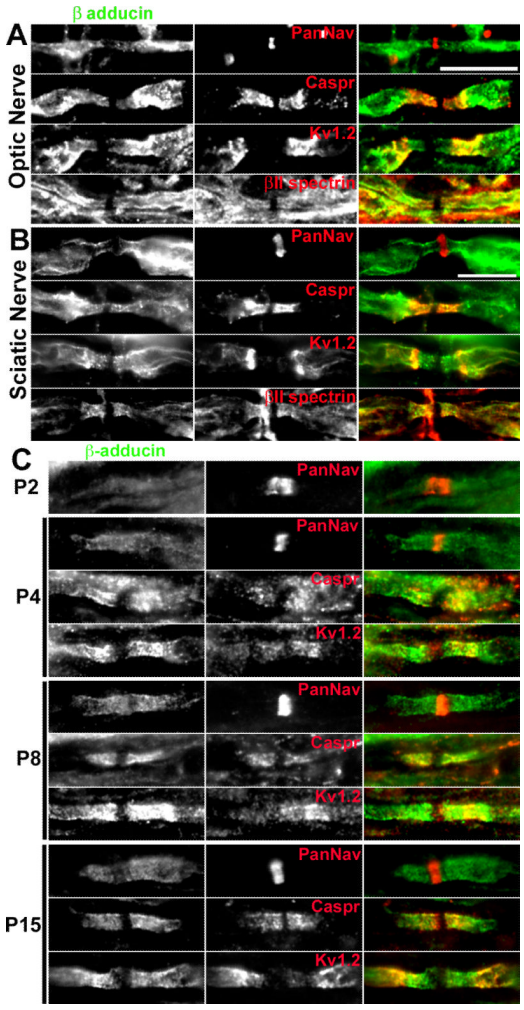

Figure 2.

β-adducin is enriched in myelinated axons at paranodes and juxtaparanodes. ***A,*** Immunostaining of rat optic (***A***) and sciatic nerves (***B***) for β-adducin and other node associated proteins (Na+ channels, caspr, Kv1.2, and βII spectrin). ***C,*** Immunostaining of developing rat sciatic nerve for β-adducin and the indicated node-associated proteins. Scale bars, 10 μm; the scale bar in ***B*** also applies to the panels shown in ***C***.

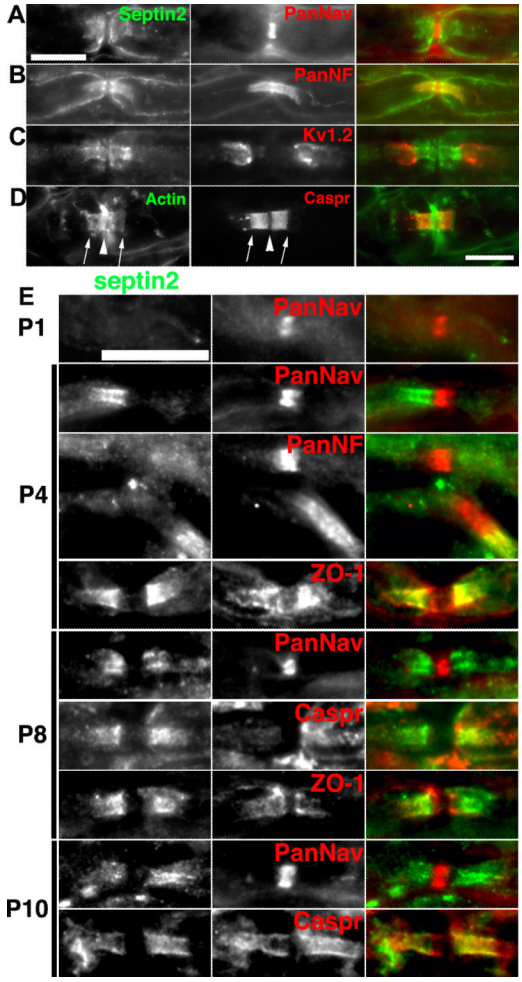

Figure 3.

Septin 2 is enriched in myelinated axons at paranodes. Immunostaining of rat sciatic for septin 2 and Na+ channels to label nodes (***A***), PanNF to label nodes and paranodes (***B***), and Kv1.2 to label juxtaparanodes (***C***). ***D,*** Consistent with septin 2′s reported role in regulating actin dynamics, immunostaining for actin reveals clear colocalization of actin with caspr. other node associated proteins (Na+ channels, caspr, Kv1.2, and βII spectrin). ***E,*** Immunostaining of developing rat sciatic nerve for septin 2 and the indicated node-associated proteins. Scale bars, 10 μm; the scale bar in ***A*** also applies to the panels shown in ***B,*** and ***C***.

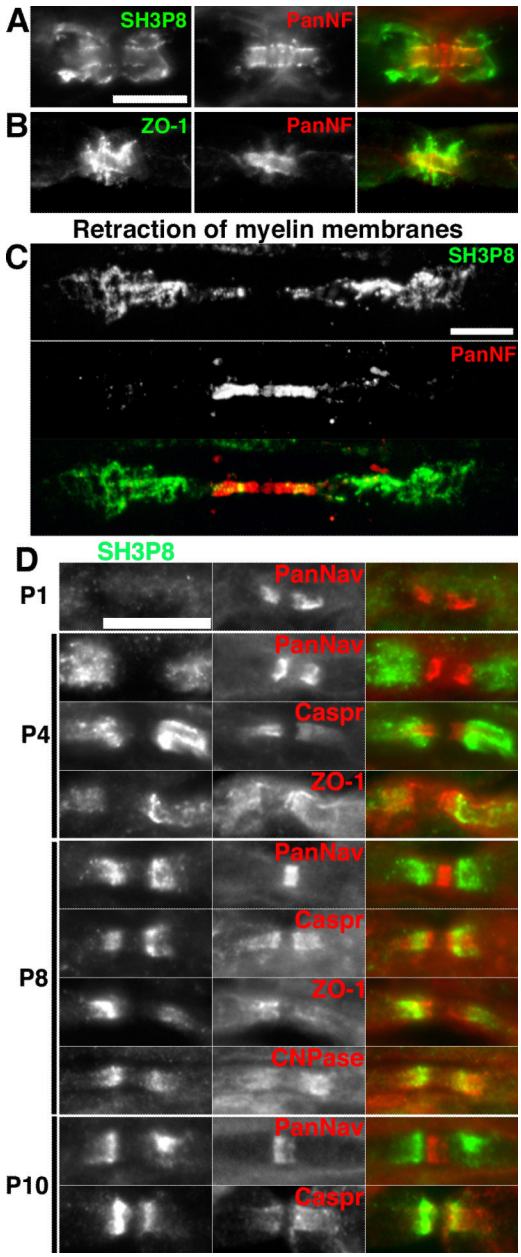

Figure 4.

Sh3p8 is enriched in Schwann cells at paranodes. ***A,*** Immunostaining of rat sciatic nerves for sh3p8 and panNF. ***B***, Immunostaining of rat sciatic nerves for ZO1 and panNF suggests sh3p8 is not a component of autotypic tight junctions. ***C,*** Retraction of Schwann cell membranes demonstrates paranodal sh3p8 is associated with Schwann cells rather than axons. ***D,*** Immunostaining of developing rat sciatic nerve for sh3p8 and the indicated node-associated proteins. Scale bars, 10 μm; the scale bar in ***A*** also applies to ***B***.

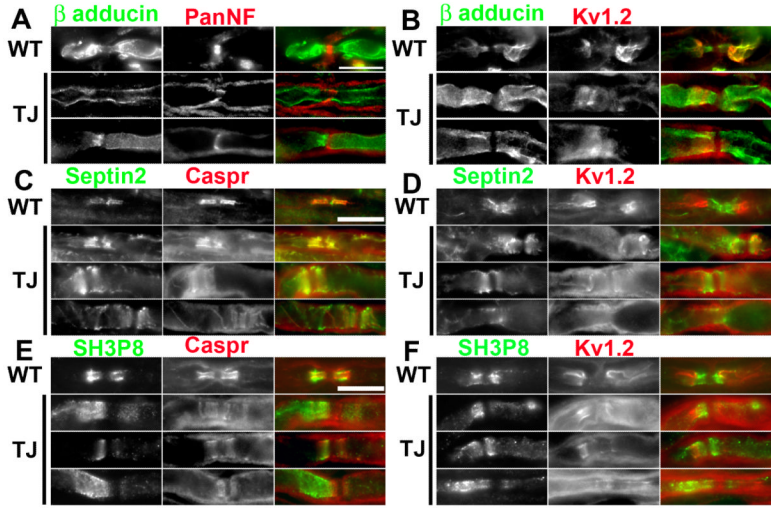

Figure 5.

β-adducin, septin 2, and sh3p8 localization is disrupted in *TremblerJ (TrJ)* dysmyelinating mutant mice. ***A, B,*** Immunostaining of sciatic nerves in WT and *TrJ* mice using antibodies against β-adducin and PanNF (***A***) or Kv1.2 (***B***). ***C, D,*** Immunostaining of sciatic nerves in WT and *TrJ* mice using antibodies against septin 2 and caspr (***C***) or Kv1.2 (***D***). ***E, F,*** Immunostaining of sciatic nerves in WT and *TrJ* mice using antibodies against sh3p8 and caspr (***E***) or Kv1.2 (***F***). Scale bars, 10 μm; the scale bars in ***A, C,*** and ***E*** apply to ***B, D,*** and ***F***, respectively.

Table 1

Putative functional classification of the 416 proteins identified by mass-spectrometry

Protein Classification	*# of proteins*	*Percentage*
cytoskeleton/scaffolds	69	16.6
membrane	40	9.6
ER/ribosomal	15	3.6
enzymes	106	25.5
anchor/adaptor	29	7.0
endo/exocytosis	38	9.1
extracellular matrix	7	1.7
motors	15	3.6
other or unknown	96	23.1